Available online at www.sciencedirect.com
ScienceDirect
ELSEVIER
European Journal of Mechanics B/Fluids 26 (2007) 707–719

Soil erosion in the boundary layer flow along a slope: a theoretical study

Olivier Brivois [a,b], Stéphane Bonelli [b,*], Roland Borghi [a,c]

[a] *Laboratoire de Mécanique et d'Acoustique (UPR-CNRS 7051), 31, chemin Joseph Aiguier, 13402 Marseille, France*
[b] *Cemagref, 3275, Route de Cezanne, CS 40061, 13182 Aix-en-Provence, Cedex 5, France*
[c] *EGIM, IMT – Technopôle de Château-Gombert, 13451 Marseille, France*

Received 10 August 2005; received in revised form 18 December 2005; accepted 19 March 2007

Available online 24 April 2007

Abstract

To better understand the phenomena involved in hydraulic erosion of soils, the influence of the eroded mass flow rate on the velocity field of the water flow is investigated by an original theoretical model. We consider the situation of a turbulent two-phase fluid flow over an erodable solid medium, with both turbulent stresses and turbulent particles diffusion in the flow. In the reference frame linked to the ground surface, the flow can be considered as a quasi-steady state and modelled by the boundary layer equations with addition of mass injection from the ground to account for erosion. To solve completely the problem, the prescription of a local erosion criterion is necessary to evaluate the local eroded mass flow rate. We consider here a purely mechanical process: the eroded flow rate is proportional to the difference between the tangential stress induced by the flow and a critical value characteristic of the soil. In this theoretical frame, we can study the influence of several parameters, as the slope of the ground or the sediments density. One of the main results obtained is the existence for a given set of the parameters of a critical slope angle separating two different erosion regimes.

Keywords: Erosion modelling; Turbulent two-phase flow; Boundary layer

1. Introduction

A large literature on sediment transport exists in the field of hydraulics [1–3]. These studies concern more the transport of the sediments than their erosion itself. In fact, most of the previous works on soil erosion or sediment transport, either experimental or theoretical, deal only with free-surface flows with weak slope situations, described by the shallow-water equations [4,5]. In this framework, the erosion flow rate, as well as the friction stress on the ground, are prescribed as a function of the height and mean velocity of water. To do that, empirical relations are implemented, and the validity of the prediction is consequently linked to the relevance of the experiments in the practical case investigated.

On the other hand, one can infer that the local friction stress induced on the ground surface by the flow is certainly a striking variable to quantify the local eroded mass flow rate. But in the same time this friction stress is itself modified

* Corresponding author. Tel.: +33 (0)4 42 66 99 53; fax: +33 (0)4 42 66 88 65.
E-mail address: stephane.bonelli@cemagref.fr (S. Bonelli).

0997-7546/$ – see front matter
doi:10.1016/j.euromechflu.2007.03.006

Nomenclature

L	length unit	
M	mass unit	
T	time unit	
D	effective diffusion coefficient (mass diffusivity)	$\mathrm{L^2\,T^{-1}}$
d_s	sediment particle diameter	L
$\vec{g}$	gravitational constant	$\mathrm{L\,T^{-2}}$
h_0	value of y where u_0 is equal to u_e	L
l_m	mixing length	L
S_C	Schmidt number	
u, v	longitudinal and transverse velocity	$\mathrm{L\,T^{-1}}$
u_0	flow inlet velocity	$\mathrm{L\,T^{-1}}$
u_e	maximum value of u_0, at the external boundary of the boundary layer	
x, y	longitudinal and transverse coordinate	L
Y	mass fraction of particles	
Y^-	mass fraction of particles in the soil	
$\underline{\underline{\delta}}$	Kronecker delta	
δ	boundary layer thickness	L
ρ, ρ_s, ρ_f	total, solid, fluid density	$\mathrm{M\,L^{-3}}$
$\underline{\underline{\tau}}$	friction stress tensor	$\mathrm{M\,L^{-1}\,T^{-2}}$
τ_c	critical shear stress to cause erosion	$\mathrm{M\,L^{-1}\,T^{-2}}$
K	coefficient of soil erosion	$\mathrm{T\,L^{-1}}$
μ_eff	effective dynamic viscosity	$\mathrm{M\,L^{-1}\,T^{-1}}$
μ_w	water molecular viscosity	

by the eroded flow rate, since the injection of particles in the flow does modify the velocity profile near the ground surface.

When erosion phenomena take place near the wall (i.e, the fluid/soil interface), those problems are often solved by integral boundary layer theory [6], or by two-dimensional boundary layer models [7]. However, few attempts have been made to model two-phase flows with erosion on a strong slope. The paper presented here is intended as a further step in this direction.

Following this introduction, Section 2 summarises the equations for diphasic flow with fluid/soil interface erosion. In Section 3, the boundary layer flow with erosion are presented. Obtained numerical results are presented and discussed in Section 4.

2. Diphasic flow with erosion modelling

2.1. The mixture balance equations

It is proposed to study the surface erosion of a fluid/soil interface subjected to a flow running parallel to the interface. The soil is eroded by the flow, which then carries away the eroded particles. For further details about the different mechanisms involved in two-phase flows, and the existing models, see for instance Savioli [8] or Sommerfeld [9]. The two-phase flow is considered as a continuum. Such an assumption for the dispersed sediment particles is acceptable if the particle size remains very small with respect to the length scale of variations in the mean flow. Here we will assume that this condition is always true.

The mass conservation equations for the water-sediment mixture and for the mass of particles as well as the balance equation of momentum of the mixture can be written as follows in an Eulerian framework [10]:

$$\partial_t \rho + \vec{\nabla}\cdot(\rho\vec{u}) = 0, \tag{1}$$

$$\partial_t(\rho Y) + \vec{\nabla}\cdot(\rho\vec{u}Y) + \vec{\nabla}\cdot\vec{J} = 0, \tag{2}$$

$$\partial_t(\rho\vec{u}) + \vec{\nabla}\cdot(\rho\vec{u}\otimes\vec{u}) = -\vec{\nabla}p + \vec{\nabla}\cdot\underline{\underline{\tau}} + \rho\vec{g}, \tag{3}$$

where ρ is the mixture density, $\vec{u}$ is the concentration-weighted average velocity, Y is the mass concentration of particles in the fluid, $\vec{J}$ is the mass diffusion of the flux of particles (due to the difference between the mean velocity of sediments particles and the one of water), p is the pressure in the mixture, $\underline{\underline{\tau}}$ is the mixture deviatoric stress tensor, and $\vec{g}$ is the vector of gravitational forces. The total density of the fluid-particle mixture ρ is given by:

$$\rho = \left(\frac{Y}{\rho_\mathrm{s}} + \frac{1-Y}{\rho_\mathrm{f}}\right)^{-1},$$

where ρ_f and ρ_s are the densities of the fluid medium and of the solid particles which are both constant. The principal unknowns in these balance equations are p, Y and $\vec{u}$. Note that here, for the two-phase mixture, these variables are defined as mean values averaged in a small volume. In this elementary volume, each fluid/solid particle has its own velocity, different from the mean value $\vec{u}$. First, because the initial or boundary conditions experienced by each particle are not the same and cannot be perfectly known, and second, because these initial perturbations are amplified by the flow, until a kind of random global saturated state, the "turbulent flow" is reached. It can be shown that these perturbations of velocities play an important role in $\underline{\underline{\tau}}$ and $\vec{J}$. For further details, see for instance [10].

2.2. The mixture behaviour laws

Simple laws for $\vec{J}$ and $\underline{\underline{\tau}}$, which represent the momentum and mass transport within the mixture, can be given by the classical irreversible thermodynamics (giving the classical approach of Boussinesq (1877)). The friction law of the mixture is therefore

$$\underline{\underline{\tau}} = 2\mu_\mathrm{eff}\,\underline{\underline{d}}. \tag{4}$$

The deviatoric strain rate tensor $\underline{\underline{d}}$ is defined as follows:

$$\underline{\underline{d}} = \frac{1}{2}\left(\vec{\nabla}\vec{u} + {}^\mathrm{T}\,\vec{\nabla}\vec{u}\right) - \frac{1}{3}\vec{\nabla}\cdot\vec{u}\,\underline{\underline{\delta}},$$

where $\underline{\underline{\delta}}$ is the second-order unit tensor, and μ_eff the so called "eddy viscosity".

The mixing process is described with a classical Fickian law. The diffusion flux is proportional to the local gradient of mass fraction:

$$\vec{J} = -\frac{\mu_\mathrm{eff}}{S_\mathrm{C}}\vec{\nabla}Y. \tag{5}$$

The Schmidt number is the ratio of the momentum and mass diffusivities, $S_\mathrm{C} = \mu_\mathrm{eff}/\rho D$, where ρD represents eddy (turbulent) mass diffusion coefficient.

In our case of turbulent diffusion of two phase flow, intuitively, both viscosity and diffusion coefficients are not constant physical properties of the mixture but should depend locally on the velocity and length scales of the turbulent fluctuations and also on the particles characteristics. In single phase turbulent flow, it is a usual assumption to consider an eddy viscosity coefficient proportional to the velocity gradient, and a Schmidt number equal to 1. This is known as the "Prandtl Mixing Length model"; see for instance [11]:

$$\mu_\mathrm{eff} = \mu_\mathrm{w} + \rho l_\mathrm{m}^2\dot{\gamma}, \qquad S_\mathrm{C} = 1, \tag{6}$$

where l_m is the mixing length and $\dot{\gamma} = \sqrt{\frac{1}{2}\underline{\underline{d}} : \underline{\underline{d}}}$ is the equivalent strain-rate.

The mixing length l_m corresponds to the relevant length scale of turbulence, then the associated velocity scale is simply $l_\mathrm{m}\dot{\gamma}$. Here we implicitly consider that the velocity gradient is the main local variable that controls the velocity scale of the turbulent field.

Bagnold introduced a similar formula in 1954 (in [12]) to describe an intensely sheared fluid-granular mixture in the collisional regime, with a mixing length simply equal to the mean grain diameter. The quadratic rheological law for hyperconcentration flows is also similar to this description [13].

The key problem is now to evaluate the mixing length. In developed sheared turbulent flows, experiments show that l_m, viewed as a characteristic scale of the "eddies" embedded in the flow, depends on the total thickness of the sheared layer, but is limited by the distance to the wall, if any. It means that this mixing length is not a strictly local variable, whereas the velocity gradient is. When the turbulent flow is a dense two phase flow, we can infer that the density field and the size of the particles have also to be taken into account. An example can be found in [14].

Out of the framework of linear irreversible thermodynamics, more detailed laws for the momentum and mass transport can be obtained from the literature of two-phase turbulent flows [15,13]. For the sake of simplification, we assume the gravitational forces to be negligible in comparison to the turbulent forces in the diffusion process: sedimentation and deposition are neglected. In particular, the model for the diffusion flux $\vec{J}$ (Eq. (5)) can be improved by including gravity effects through the "terminal velocity" [13].

These behaviour laws are somewhat basic, but they yield a simple description of the time-averaged behaviour of a diphasic turbulent flow. Sophisticated models are possible [15,8]. Although turbulence models of considerable sophistication are now commonly used in single-phase fluid flows, the same cannot be said for the two-phase flow involving heavy particles of varying concentration.

2.3. The interface balance equations

The two media, i.e. the solid ground and the two-phase fluid, are separated by an interface Σ or the ground surface. Erosion of the ground induces a mass flux across this interface and in the same time the eroded matter undergoes a transition from solid-like to fluid-like behaviour. Above the ground interface, the water-particle mixture is assumed to flow as a fluid, while a solid-like behaviour is considered underneath. This interface constitutes, to the lowest order of approximation, a discontinuity location. To state how the two-phase systems behave as the interface is crossed is the core of the present erosion model.

A rigorous theory for internal boundaries has been developed by [16]. Let $\vec{n}$ be the normal unit vector of Σ oriented outwards the solid-like region. At a position x located along Σ, we distinguish between the quantities a^+ and a^- belonging respectively to the fluid and the solid side. The following points must be emphasised:

(1) the solid–fluid interface Σ is not a material interface, but a purely geometric separation (it has no thickness on its own);
(2) Σ can move with a velocity $\vec{v}_b$ oriented in the normal direction $\vec{n}$, so $\vec{v}_b = v_b\vec{n}$;
(3) the motion of Σ accounts for the erosion process so the boundary conditions must deal with the flux balances on Σ.

To guarantee equivalence between the inner and the outer quantities, the Rankine–Hugoniot or Hadamard equations expressing local conservation laws across a discontinuity are used:

$$\left[\rho(\vec{u} - \vec{v}_b) \cdot \vec{n}\right]_-^+ = 0, \tag{7}$$

$$\left[\rho Y(\vec{u} - \vec{v}_b) \cdot \vec{n} + \vec{J} \cdot \vec{n}\right]_-^+ = 0. \tag{8}$$

The eroded material that comes from the solid medium is equal to the one that enters the liquid medium, as expressed in Eq. (7). The total flux of eroded material (both water and sediment) $\dot{m}$ is defined as follows:

$$\dot{m} = \rho^-(\vec{u}^- - \vec{v}_b) \cdot \vec{n} = \rho^+(\vec{u}^+ - \vec{v}_b) \cdot \vec{n}. \tag{9}$$

As a consequence, relatively to the interface, a density jump of the material implies also a velocity jump (for instance when the eroded particles are denser than the “solid” ground, which contains also water).

The soil is assumed to be rigid ($\vec{u}^-$ is uniform), saturated and devoid of seepage ($\vec{J}^- = 0$), and homogeneous (ρ^- is uniform, or equivalently Y^- is uniform). As a consequence, Eq. (8) leads to a mixed boundary condition for the particles mass fraction:

$$\dot{m}(Y^+ - Y^-) + \vec{J}^+ \cdot \vec{n} = 0. \tag{10}$$

Of course, all those hypothesis may be removed one after the other, complicating more and more the model. In particular, if the behaviour of the soil is considered (e.g. deformation behaviour law or failure criterion), the jump equation of the mixture momentum conservation shoul be included: this equations relates at the interface the stresses in the fluid to the stresses in the ground.

The interface velocity $\vec{v}_b$ is one of the unknowns of the problem and, in a frame attached to the solid ($\vec{u}^- = 0$ in the solid medium), it is then given by:

$$\vec{v}_b = -\frac{\dot{m}}{\rho^-}\vec{n}.$$

The mass of eroded particles which cross the interface per unit of area and per unit of time, q_s, is defined by $q_s = Y^-\dot{m}$. An additional behaviour model of erosion is necessary to determine $\dot{m}$, i.e. to describe the interface velocity.

2.4. The interface behaviour law

Erosion laws dealing with soil surface erosion by a tangential flow are often written in the form of threshold laws such as:

$$\dot{m} = \begin{cases} 0 & \text{if } |\tau_\mathrm{b}| < \tau_\mathrm{c}, \\ K(|\tau_\mathrm{b}| - \tau_\mathrm{c}) & \text{otherwise,} \end{cases} \tag{11}$$

where τ_c is the critical shear stress [17,10,18], and K is the erodibility rate [17]. In Eq. (11) τ_b is the tangential stress on fluid side of the interface defined by:

$$|\tau| = \sqrt{(\underline{\underline{\tau}} \cdot \vec{n})^2 - (\vec{n} \cdot \underline{\underline{\tau}} \cdot \vec{n})^2}.$$

This erosion law dates back a long way. It was first used to in studies of free-surface flows [1,19]. We have used the same law for a our flow: this constituted the choice of the behaviour law of the fluid/soil interface.

For a non-cohesive granular soil, τ_c is simply linked to the critical Shields number θ, $\tau_\mathrm{c} = \theta g d_\mathrm{s}(\rho_\mathrm{s} - \rho_\mathrm{f})$ where d_s is the mean particle size and $\theta \approx 0.05$. For a cohesive soil, τ_c can equally be referred to as a critical shear stress for erosion, in analogy with cohesionless sediment transport [19]. A typical value, chosen below, is $\tau_\mathrm{c} = 10$ Pa. Laboratory experiments performed by Ariathurai and Arulanandan [17] and Wan and Fell [20] found values of K in the range of 10^{-5}–10^{-2} s/m. There is no equivalent value of K for non-cohesive soil.

The normal stress, its mean value and fluctuations are other parameters that could possibly be taken into account. The critical shear stress may depend on the solid ground characteristics as its water content or its microscopic structure.... The linear law Eq. (11) can be considered as a first order expansion.

A special case of the erosion law corresponds to an infinite value of K. In this case, one gets unilateral conditions on Σ:

$$|\tau_\mathrm{b}| - \tau_\mathrm{c} \leqslant 0, \quad \dot{m} \geqslant 0, \quad \dot{m}\big(|\tau_\mathrm{b}| - \tau_\mathrm{c}\big) = 0. \tag{12}$$

Then, when erosion occurs, the shear stress remains equal to τ_c while the eroded mass flow adapts its value.

3. Boundary layer flow with erosion

3.1. The mixture balance equations

Complete Navier–Stokes computation is nowadays accurately achieved through numerical solvers. Nevertheless, some simplifications are physically acceptable and expedient. A simplified description provides a better understanding of the phenomena and relevant scalings. In order to analyse the behaviour of our simple model, the study will be limited to the case of elongational and dilute flow approximation. This set of equations was previously used to study piping erosion in soils [21]. The use of these equations is extended here to the study of two-phase boundary flow with erosion on steep slope.

We adopt in the following a co-ordinate system linked to the interface, in which the x-axis is oriented in the streamwise direction, and the y-axis in the transversal direction, upward and perpendicular to the interface (Fig. 1). In this way, the interface is always at $y = 0$. This choice allows to only include the fluid-like material inside the control volume. Consequently the co-ordinate system moves when the interface is eroded, and, the inertial force due to this movement, i.e. the acceleration, is neglected. This way, the system can be considered in a quasi-steady state regime.

This approximation can be used when the interface is plane or weakly curved, and when any variation in the horizontal direction is small enough compared with the transverse variation.

For this two-dimensional flow over a semi-infinite flat plate, Eqs. (1)–(8) can be non-dimensionalised by the dynamical boundary layer scales. By estimating the order of magnitude of each term of these dimensionless equations [24], we obtain the elongational flow approximation in which case the governing equations are

$$\frac{\partial}{\partial x}(\rho u) + \frac{\partial}{\partial y}(\rho v) = 0, \tag{13}$$

$$\frac{\partial}{\partial x}(\rho Y u) + \frac{\partial}{\partial y}(\rho Y v) = \frac{\partial}{\partial y}\left(\frac{\mu_\mathrm{eff}}{S_\mathrm{c}}\frac{\partial Y}{\partial y}\right), \tag{14}$$

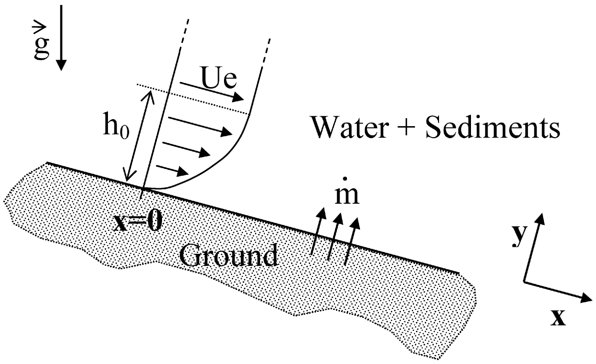

Fig. 1. The flow configuration.

$$\frac{\partial}{\partial x}\left(\rho u^2\right)+\frac{\partial}{\partial y}(\rho u v)=-\frac{\partial p}{\partial x}+\frac{\partial}{\partial y}\left(\mu_{\text{eff}}\frac{\partial u}{\partial y}\right)+\rho g\sin\alpha, \tag{15}$$

$$0=\frac{\partial p}{\partial y}+\rho g\cos\alpha, \tag{16}$$

where α is the angle between the x-axis and the horizontal direction ($\alpha \geqslant 0$).

These equations are similar to the Reduced Navier–Stokes/Prandtl equations [7]. The flow has a streamwise component u and a transverse component v, while the diffusion flux has only a transversal component, and the stress has only a shear component. However, the pressure gradient in the transverse direction is not negligible, as in the classical boundary layer equations.

3.2. The boundary conditions

The entry and boundary conditions are as follows:

$$u(0,y)=u_0(y), \qquad Y(0,y)=0, \tag{17}$$

$$v(x,0)=\frac{\dot m}{\rho^+}, \qquad -\frac{\mu_{\text{eff}}}{S_C}\frac{\partial Y}{\partial y}(x,0)=\dot m\left(Y^- - Y(x,0)\right), \tag{18}$$

$$u(x,0)=0, \qquad \lim_{y\to\infty}u(x,y)=u_e, \qquad \lim_{y\to\infty}Y(x,y)=0, \tag{19}$$

where the subscript e denotes the values out of the boundary layer.

As the solid ground is rigid and devoid of seepage, the longitudinal velocity component is zero on the ground, but not the transverse component, which is prescribed by the erosion law. Of course, when the erosion velocity is much more lower than of the flow velocity, this transverse component may be neglected for calculating $u(x,y)$, as in [7]. However, the actual relevant boundary conditions are (17), (18) and (19).

3.3. The pressure gradient

The longitudinal pressure gradient has also to be prescribed in order to integrate the set of equations. This gradient is only due to the flow outside the boundary layer, and depends on the flow configuration. The simplest case that can be considered is a zero pressure gradient.

For a very large height of water, Eq. (16) gives, after derivation with respect to x:

$$\frac{\partial p}{\partial x}=\frac{\partial p}{\partial x}(x,0)-(\rho_f g\cos\alpha)\frac{\partial}{\partial x}\int_0^y\left(\frac{\rho}{\rho_f}-1\right)\mathrm{d}y'. \tag{20}$$

Expressing Eq. (20) at very large y, with help of Eq. (15), gives:

$$\frac{\partial p}{\partial x} = \underbrace{-\rho_{\mathrm{f}} u_{\mathrm{e}} \frac{\mathrm{d}u_{\mathrm{e}}}{\mathrm{d}x}}_{\mathrm{I}} + \underbrace{\rho_{\mathrm{f}} g \sin\alpha}_{\mathrm{II}} + \underbrace{(\rho_{\mathrm{f}} g \cos\alpha) \frac{\partial}{\partial x} \int_{y}^{\infty} \left(\frac{\rho}{\rho_{\mathrm{f}}} - 1 \right) \mathrm{d}y'}_{\mathrm{III}}. \tag{21}$$

This last formula underlines the influences of the external velocity gradient (term I) and the slope (term II), as well as the density of the sediments (term III).

When $\partial p/\partial x$ is given, the set of equations is a parabolic one, and can be integrated marching downstream. However, the set of equations, including (21) is no more parabolic, because the downstream influence is embedded in $\partial/\partial x$. The effect of the last term is nearly similar to the ones observed in the "mixed convection problem" in buoyant flows [22,23].

3.4. The behaviour laws

The elongational flow approximation leads to:

$$\tau = \mu_{\mathrm{eff}} \frac{\partial u}{\partial y}, \qquad \dot{\gamma} = \left| \frac{\partial u}{\partial y} \right|.$$

As usual for single phase turbulent flow, the mixing length is calculated with $l_{\mathrm{m}} = \min(0.1\delta, 0.435y)$ where δ is the boundary layer thickness.

In the turbulent boundary layer, the laminar sublayer is more or less thick depending on the fluid molecular viscosity μ_{w} and on the roughness of the wall. In our case, the ground roughness may be very significant because its geometrical scale is about the mean size of the particles eroded from the ground. The influence of wall roughness on the laminar sublayer and, consequently, on the shear stress at the wall has been studied in details [24]. The classical formulae proposed for this sublayer is used here with a roughness of the order of 1 mm.

4. Results

The simple problem shown on Fig. 1 will be considered. The principle of the numerical method used to solve the previous equations is shortly presented in Appendix A. The numerical procedure for solving the system with the erosion law Eq. (12) is described in Appendix B.

The parameters chosen for numerical calculations are listed in Table 1. The exterior velocity u_{e} is kept constant for all the calculations: the term I of Eq. (21) is zero. The total height of water above the ground is very large, but the boundary layer, where the velocity gradient is non-zero, is finite: its initial value is h_0 at the upstream position ($x = 0$) and increases with x. The choice of the velocity profile at $x = 0$ may be arbitrary. It will influence the erosion at small x. However, it is a well known fcat in classical boundary layers without gravity that the velocity profile tends toward a self-similar shape, depending only on h_0 and u_{e}. In our calculations, the erosion is activated only downstream the abscissa $x = x_{\mathrm{c}}$, where this classical self-similar turbulent boundary layer profile is obtained.

The thickness of the velocity gradient layer at $x = x_{\mathrm{c}}$ is noted δ_0. We introduce the dimensionless variables:

Table 1
Model parameters used in application

$u_{\mathrm{e}} = 3.5$ m/s,	$h_0 = 0.1$ m
$\rho_{\mathrm{f}} = 1000$ kg/m^3,	$Y^- = 0.6$
$\tau_{\mathrm{c}} = 10$ Pa	

Nota: 1 Pa = 1 kg m^{-1} s^{-2}; and Y^- is the solid mass fraction of the ground.

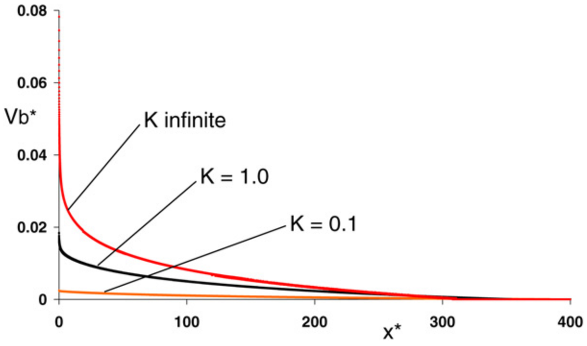

Fig. 2. Ground regression velocity for 3 values of K.

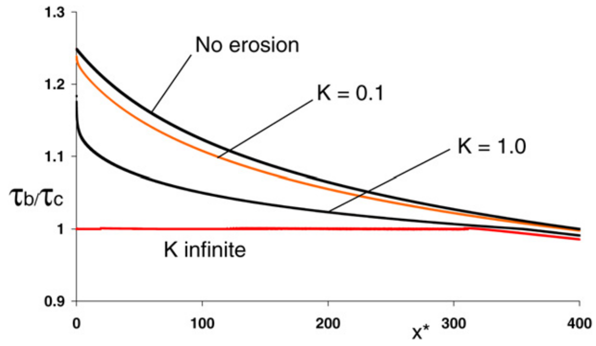

Fig. 3. Shear stress on the ground for 3 values of K, and with no erosion.

$$x^* = \frac{x - x_c}{\delta_0}, \quad y^* = \frac{y}{\delta(x)}, \quad U^* = \frac{u}{u_e}, \quad Y^* = \frac{Y}{Y^-},$$
$$\tau_c^* = \frac{\tau_c}{\rho_f u_e^2}, \quad K^* = K\sqrt{\frac{\tau_c}{\rho_f}}, \quad \rho_s^* = \frac{\rho_s}{\rho_f}, \quad v_b^* = v_b\sqrt{\frac{\rho_f}{\tau_c}}.$$

To analyse the phenomena, it is convenient to consider separately the influence of the density of sediments and the slope of the ground.

4.1. Erosion on an horizontal ground with neutrally buoyant sediments

We consider an horizontal ground ($\alpha = 0$ so the term II of Eq. (21) is zero), and neutrally buoyant sediments ($\rho_s = \rho_f$ so the term III of Eq. (21) is zero). The horizontal pressure gradient is therefore zero.

Fig. 2 shows the ground regression velocity versus x^* for three values of K. Obviously for a given value of τ_c, the larger is K, the larger is the local eroded mass flow rate, i.e. the ground regression velocity. At the starting point of the erosion ($x^* = 0$), the regression velocity is relatively high and decreases with x^*, until it becomes zero near $x^* = 300$. In this situation, the erosion is finite in distance (and in quantity). The shear stress on the ground is shown on Fig. 3 for the same calculation than Fig. 2 and for no erosion condition. This last curve, labelled “No erosion”, corresponds to the same hydraulic condition, but in this case the soil is considered as not erodable (its critical shear stress is very high). From this figure, we observe that for weak values of K (<0.1 s/m), the shear stress on the ground is quite the same as in the no erosion case, but for stronger values of K, the erosion causes a decrease of the shear stress. For the infinite value of K, the shear stress on the ground during erosion is equal to τ_c.

As the outside velocity of the boundary layer is constant and equal to $u_e = 3.5$ m/s, the shear stress on the ground decreases, due to the development of the thickness of the layer. In addition, if the local eroded mass flow rate is high enough, the erosion also reduces the shear stress on the ground. This phenomenon is well known for single phase flows [24]: mass injection at the wall reduces the shear stress. This can be seen on Fig. 4, where the evolution of the velocity profiles due to erosion is presented. The first profile, at $x^* = 0 - eps$, is the classical self-similar turbulent boundary layer one and we clearly see its deformation due to the eroded flux through the wall (note that to increase these effects, we have chosen here the infinite value of K and $\tau_c = 5$ Pa).

The evolution of the thickness of the boundary layer versus x^* is presented on Fig. 5, for three values of K and with no erosion. Of course the inflow of eroded matter increases the thickness of the layer, and tends to decrease again the shear stress on the ground.

A typical evolution of the mass fraction profile along the flow is shown on Fig. 6. The curve at $x^* = 0$ corresponds to the very beginning of erosion, and the mass fraction of sediment, Y, is so relatively important near the boundary, and null elsewhere. Downstream, for small x^*, Y at the ground first increases, to reach a maximum near $x^* = 35$, then decreases, due to the decrease of the local eroded mass flow rate, at $x^* = 180$. Along this distance, the eroded sediments go on spreading in the layer, increasing its mass fraction. Then, after the erosion had stopped, near $x^* = 300$, the mass fraction decreases into the layer, due to the diffusion of the sediments and to the inflow of pure water coming from the top of the layer.

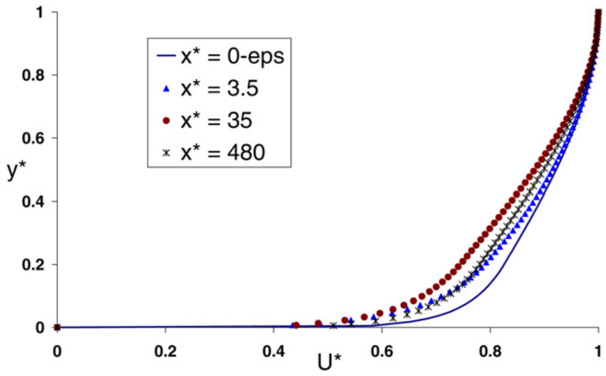

Fig. 4. Velocity profiles evolution, for K infinite and $\tau_c = 5$ Pa.

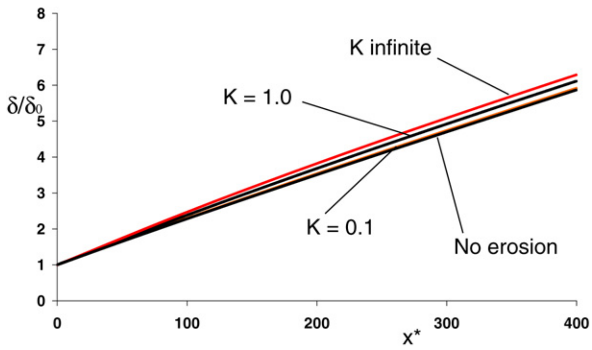

Fig. 5. Boundary layer thickness evolution for 3 values of K and no erosion, $\tau_c = 10$ Pa.

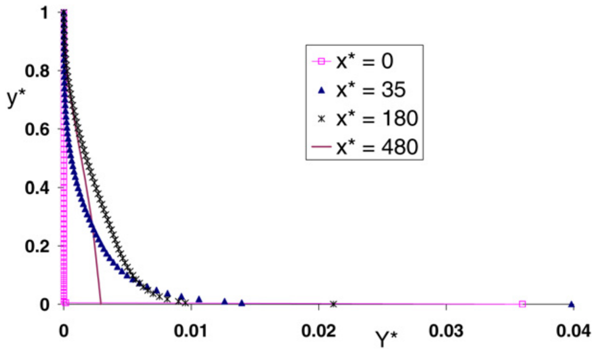

Fig. 6. Mass fraction of sediments evolution for $K = 0.1$ s/m.

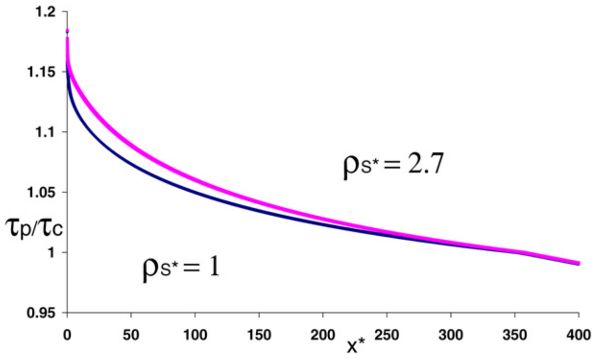

Fig. 7. Shear stress on the ground versus x^* for two values of ρ_s^*.

To sum up, the main results obtained here are: (1) the erosion induces a shear stress decrease on the ground; (2) for an horizontal ground with a constant external velocity, the erosion is finite in distance and in quantity.

4.2. Erosion on an horizontal ground with sedimentsdenser than fluid

We consider this time sediments denser than fluid ($\rho_s > \rho_f$). The horizontal pressure gradient is therefore given by the term III of Eq. (21). The evolution of the shear stress on the ground versus x^* is presented on Fig. 7 for two sediment densities, namely $\rho_s^* = 1$ and $\rho_s^* = 2.7$. The parameters are the same as before, with $K = 0.1$ s/m. One can clearly see that an increase of the sediments density increases the shear stress on the ground (and so the local eroded mass flow rate).

This increase with the sediments density cannot be explained by the pressure gradient effect. In fact, we have seen that this pressure gradient involves a term linked to the variation of the density in the flow due to transverse gravity effect. And, when the mass fraction of sediments increases in the flow due to erosion (we have already talked about this with Fig. 6), this latter (source) term is negative since $\rho_s^* > 1$, and tends consequently to slow down the flow. So only an increase of the momentum, or of the viscosity, near the ground, induced by the presence of the eroded sediments can explain this effect.

The influence of the sediments density remains weak and cannot be clearly seen on velocity or mass fraction profiles. As the erosion stays finite, for a non-inclined ground, we can look at the global eroded mass flow rate calculated as: $Q_e = \int_0^{+\infty} \dot{m}\, dx^*$. We then define $Q_e^* = Q_e/(\rho_f u_e \delta_0)$.

This global eroded mass flow rate is presented in Fig. 8 versus the density ratio ρ_s^*. On this figure, we have plotted several curves corresponding to different values of K. For the K infinite curves, the viscosity is calculated with the water density as $\mu_{eff} = \mu_w + \rho_f l_m^2 |\partial u/\partial y|$ ("K infinite water") or with the local mixture density as $\mu_{eff} = \mu_w + \rho l_m^2 |\partial u/\partial y|$ ("K infinite mixture"). So the increase of the local mixture density induces mainly an increase of

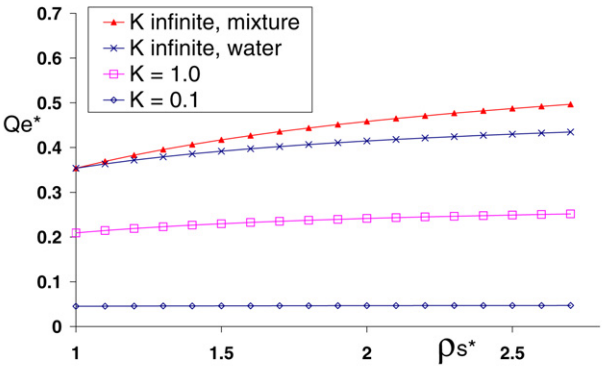

Fig. 8. Total eroded mass flow rate versus density of sediments.

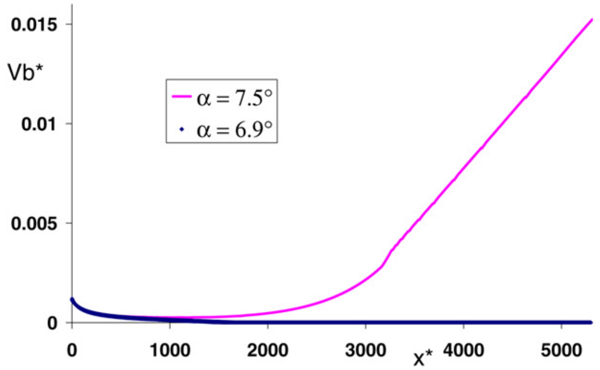

Fig. 9. Ground velocity regression for two slope angles just beneath and below the critical angle, $K = 0.1$ s/m.

the momentum and of the viscosity in a smaller extent. We can notice that for small values of K, the eroded mass flow rate is so weak that the presence of sediments plays no role in the flow (the global eroded mass flow rate remains quite constant with the sediment density).

The influence of the eroded sediments density has also been studied with a constant viscosity model. Surprisingly, the results obtained in that case are the opposite of the previous results for the mixing length model: an increase of the sediments density decreases the shear stress on the ground and so the local and global eroded mass flow rates. Indeed, this decrease of the shear stress on the ground is due to the pressure gradient effect. With a constant viscosity, the self-similar velocity profile is the Blasius one; due to its shape, this velocity profile is relatively sensitive to negative pressure gradient. And the local increase of the density near the ground is not sufficient to balance the decrease of the momentum by the pressure gradient. Moreover, when a sufficiently large quantity of matter is eroded, which creates important density gradients in the longitudinal direction, boundary layer separations has been observed ([22] or [23]).

4.3. Erosion on an inclined ground with sedimentsdenser than fluid

In this part, the density ratio is kept equal to 2.7 and the others parameters remain unchanged. We now focus on the effect of the ground slope on the erosion. As shown in Eqs. (15) and (21), the ground slope appears in the momentum balance through the term $(\rho - \rho_f)\sin\alpha$. Where the erosion occurs, the mixture density increases ($\rho > \rho_f$), so that latter term becomes positive and tends to accelerate the flow.

Consequently, the erosion increases with the slope in quantity and in distance. And for a given set of the parameters, there is a critical slope of the ground which separates two distinct erosion behaviours. Beneath this critical slope, the erosion remains finite, in distance and in quantity, as in the case of an horizontal ground. But above this slope, the erosion becomes unlimited, and, after a certain distance, increases constantly in the downstream direction. This can be seen on Fig. 9, where the ground velocity regression is shown for two slope angles, just below and above the critical slope. At the beginning of the erosion zone the two curves decrease in the same way as observed for an horizontal ground. But contrary to the curve with the angle below the critical value, the one with the angle above it does not vanish but stabilises on a certain distance before strongly rising.

For these two slope angles, we also present the corresponding velocity and mass fraction profiles on Figs. 10–13.

On Fig. 10 the velocity profiles are slightly accelerated due to the presence of sediments in the flow under the action of the longitudinal component of gravity. On Fig. 11 the mass fraction profiles are qualitatively similar to the one on Fig. 6: the erosion takes place on a finite distance, and the mass fraction remains relatively weak in the flow.

Fig. 12 shows the evolution of the velocity profiles above the critical angle. We easily understand that the increase of both the shear stress and the erosion is due to the strong acceleration of the flow under the longitudinal gravity effect. On Fig. 13 the mass fraction of the sediments continually increases with the longitudinal distance, and the mixture will become a kind of mud flow that cannot be correctly modelled by the behaviour laws chosen before.

The value of the critical slope angle versus K is presented on Fig. 14. As the eroded mass flow rate increases with the K value, the slope angle necessary to sufficiently accelerate the flow, to initiate a transition of the erosion from a limited to an unlimited regime, is all the more small if K is large.

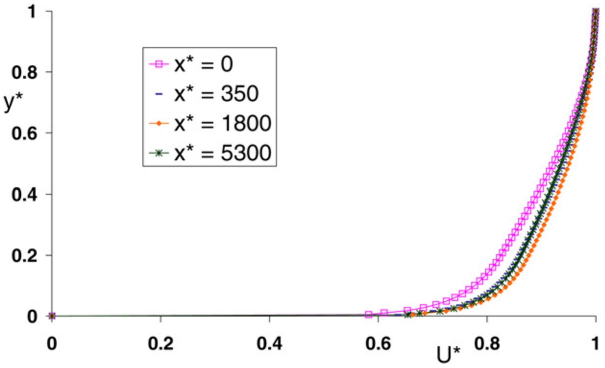

Fig. 10. Velocity profiles evolution beneath the critical angle, $K = 0.1\ \mathrm{s/m}$.

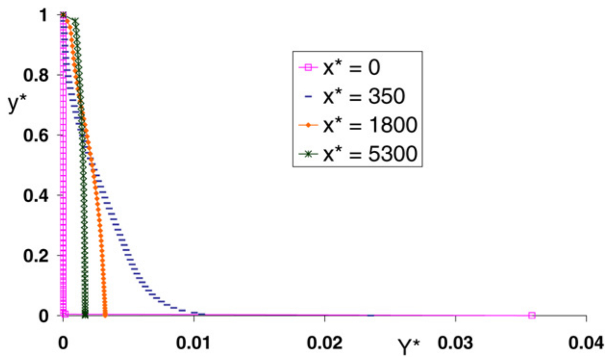

Fig. 11. Mass fraction of sediments profiles evolution beneath the critical angle, $K = 0.1\ \mathrm{s/m}$.

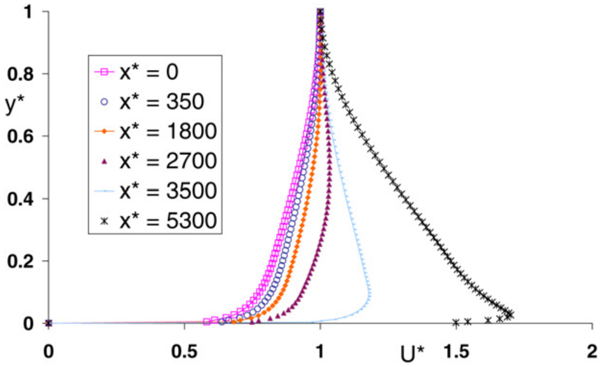

Fig. 12. Velocity profiles evolution above the critical angle, $K = 0.1\ \mathrm{s/m}$.

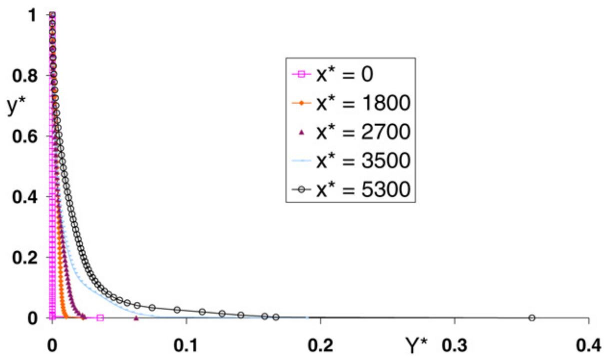

Fig. 13. Mass fraction of sediments profiles evolution above the critical angle, $K = 0.1\ \mathrm{s/m}$.

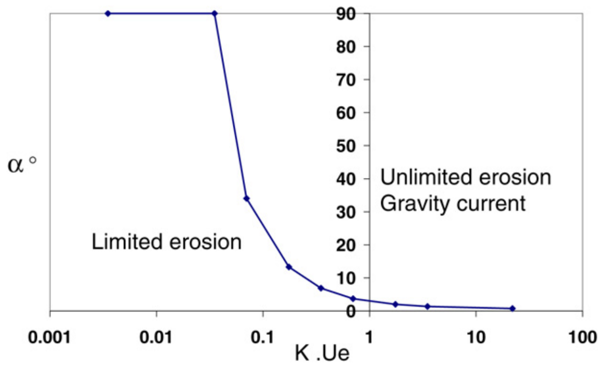

Fig. 14. Critical angle versus $K * Ue$.

Obviously, in this unlimited erosion regime, our assumption of dilute sediment suspension is no longer valid and should be improved. In particular, $\vec{J}$ and $\underline{\underline{\tau}}$, the momentum and mass transport within the mixture formulations must be modified to take into account the important quantity of sediments in the flow. Moreover, our erosion law could be no longer valid too, in denser flows.

5. Conclusion

In this paper, we propose a theoretical study of hydraulic erosion, considered as a local process. Our model, rather simple, is based on three ingredients: two-phase turbulent field equations, Rankine–Hugoniot relations at the interface, and a local erosion law. Numerical calculations are performed in a particular flow configuration: a boundary layer flow with constant exterior velocity, in a quasi-steady state situation with respect to the surface of the ground.

The existence of a strong coupling between the fluid flow, the erosion and the eroded suspended matter is underlined. Indeed, the erosion, considered as a mass injection through the interface, induces a decrease of the shear stress on the ground. Once eroded, the sediments influence the erosion process according to their density. The two components of gravity play an important role: the transverse gravity effect tends to slow down the flow while for an inclined ground, the longitudinal gravity component can induce an acceleration of the flow that strongly increases the erosion rate in the downstream direction.

The model presented here is a first approach, which needs to be improved. The closure assumptions are the simplest ones, and remain true only for dilute suspensions. So it would be necessary to better describe the interactions between the turbulence and the sediments particles, notably in the definition of the mixing length for denser two-phase mixtures. The erosion law can also be improved, for example by taking into account the normal stress applied on the ground and the soil water content.

This study is purely theoretical, and these results should be compared with experiments. Unfortunately, there is still no experimental work comparable with this particular configuration. It appears also that our model, by its use facility, could be used as a practical research tool for the testing of new physical assumptions or new theoretical approaches.

Acknowledgements

We thank the "Provence Alpes Cote d'Azur" Region for its financial support.

Appendix A. Numerical solutions

The balance equations (13)–(15) can be classically solved with the method of Spalding and Patankar [25], which first discretises the PDE in the transverse dimension by a centred finite volume scheme and then along the longitudinal dimension by an implicit Crank–Nicholson scheme. In addition, this method uses the stream function ψ as intermediate variable, and defines a new quantity, ω, to be used instead of the transverse geometrical coordinate y. ω is defined as:

$$\omega = \frac{\psi - \psi_i(x)}{\psi_e(x) - \psi_i(x)},$$

and is always between 0 and 1. $\psi_i(x)$ is the value of the stream function along the ground interface, that is: $\frac{d\psi_i}{dx}(x) = \dot{m}(x)$. $\psi_e(x)$ is the value at the external boundary of the boundary layer, defined as the zone where significant gradients of u or Y exist in the flow. It can be adjusted step by step along x.

The boundary conditions are also discretized and applied implicitly at each step in x. In the case where the erodibility rate K is infinite, $\dot{m}$ is obtained by an iterative calculation at each step (Appendix B).

The solution, i.e. u, v and Y, is considered as function of x and ω, and is obtained marching in x, and then the transverse position y is calculated following the definition of the stream function ψ:

$$y(x,\omega) = \big(\psi_e(x) - \psi_i(x)\big) \int_0^{\omega} \frac{d\omega'}{\rho(x,\omega')u(x,\omega')}.$$

Appendix B. Iterative procedure for the calculation of the local eroded mass flow rate with infinite *K*

At each space step, we are looking for a local eroded mass flow rate which effects on the flow will lead the shear stress on the ground equal to τ_c. This must be done with an iterative procedure, if k is the iteration subscript on the $\dot{m}$ calculation, we want $\dot{m}_k$ such as:

$$f(\dot{m}_k) \equiv \tau_p(\dot{m}_k) - \tau_c = 0.$$

To initialise the iterative procedure, we need two values of $\dot{m}$ and for each value the corresponding shear stress got $\tau_p(\dot{m})$. In fact for the first $\dot{m}$, called $\dot{m}_1$, any positive value is acceptable, but it is possible to find, from equations used in our problem, a first approximation that allows us to accelerate the convergence of the calculation of $\dot{m}$.

From $\dot{m}_1$, we calculate the corresponding $\tau_p(\dot{m}_1)$. Then we choose $\dot{m}_2$ as:

$$\begin{cases} \text{if } \tau_p(\dot{m}_1) > \tau_c, \text{ then } \dot{m}_2 = \dot{m}_1 + r\dot{m}_1, & 1 > r > 0, \\ \text{if } \tau_p(\dot{m}_1) < \tau_c, \text{ then } \dot{m}_2 = \dot{m}_1 - r'\dot{m}_1, & 1 > r' > 0. \end{cases}$$

From this second value of the local eroded mass flow rate $\dot{m}_2$, we calculate the corresponding shear stress got on the ground $\tau_p(\dot{m}_2)$. Once these first 4 values obtained, we can converge on the solution using the secant algorithm:

$$\dot{m}_{k+1} = \dot{m}_k - \frac{f(\dot{m}_k)}{f'(\dot{m}_k)}, \qquad f'(\dot{m}_k) = \frac{\tau_b(\dot{m}_k) - \tau_b(\dot{m}_{k-1})}{\dot{m}_k - \dot{m}_{k-1}}.$$

We then stop the iterative procedure when

$$\frac{|\tau_b(\dot{m}_k) - \tau_c|}{\tau_c} < Tol,$$

with a tolerance $Tol = 10^{-6}$.

References

[1] H. Chanson, The Hydraulics of Open Channel Flows: An Introduction, Butterworth–Heinemann, Oxford, UK, 1999.
[2] W.H. Graf, Hydraulics of Sediment Transport, McGraw-Hill, 1971.
[3] M.S. Yalin, Mechanics of Sediment Transport, third ed., Mc Graw-Hill, London, 1977.
[4] V.P. Singh, P.D. Scarlatos, Analysis of gradual earth-dam failure, J. Hydraulic Engrg. 114 (1) (1988) 21–42.
[5] V.P. Singh, Dam Breach Modelling Technology, Water Science and Technology Library, Kleiwer Academic Publishers, 1996.
[6] J. Akiyama, H. Stefan, Turbidity current with erosion and deposition, J. Hydraulic Engrg. 111 (12) (1985).
[7] P.-Y. Lagrée, Erosion and sedimentation of a bump in fluvial flow, C. R. Acad. Sci., Ser. IIb 328 (2000) 869–874.
[8] J.C. Savioli, Turbulence and sediment transport: a numerical investigation, Ph.D. Thesis, University of Twente, The Netherlands, 2000.
[9] M. Sommerfeld, Overview and Fundamentals, in: Theoretical and Experimental Modeling of Particulate Flow: Lecture Series 2000-06, VKI for Fluid Dynamics, 2000.
[10] R.I. Nigmatulin, Dynamics of Multiphase Media, Book News, Inc., Portland, OR, 1990.
[11] H. Tennekes, J.L. Lumley, A First Course on Turbulence, third ed., The MIT Press, Cambridge MA, 1974.
[12] M.L. Hunt, R. Zenit, C.S. Campbell, C.E. Brennen, Revisiting the 1954 suspension experiments of R.A. Bagnold, J. Fluid Mech. 452 (2002) 1–24.
[13] P.-Y. Julien, Erosion and Sedimentation, Cambridge University Press, 1995.
[14] A.E. Kovacs, Prandtl's mixing length concept modified for equilibrium sediment-laden flows, J. Hydraulic Engrg. 124 (8) (1998) 803–812.
[15] P. Fevrier, Etude numérique des effets de concentration preferentielle et de correlation spatiale entre vitesse de particules solides en turbulence homogène isotrope stationnaire, Ph.D. Thesis, I.N.P.G., France, 2000.
[16] L. Graziano, A. Marasco, Balance laws for continua with an interface deduced from multiphase continuous models with a transition layer, Int. J. Engrg. Sci. 39 (2001) 873–896.
[17] R. Ariathurai, K. Arulanandan, Erosion rates of cohesive soils, J. Hydraulics Division ASCE 104 (2) (1978) 279–283.
[18] A.J. Raudkivi, Loose Boundary Hydraulics, A.A. Balkema, Rotterdam/Brookfield, 1998.
[19] E. Partheniades, Erosion and deposition of cohesive soils, J. Hydraulics Division ASCE 91 (1965) 105–139.
[20] C.F. Wan, R. Fell, Investigation of rate of erosion of soils in embankment dams, J. Geotech. Geoenv. Engrg. 130 (4) (2004) 373–380.
[21] S. Bonelli, O. Brivois, R. Borghi, On the modelling of piping erosion, C. R. Acad. Sci. Paris, Ser. I 334 (2006) 555–559.
[22] H. Steinrück, Mixed convection over a cooled horizontal plate: non-uniqueness and numerical instabilities of the boundary-layer equations, J. Fluid Mech. 278 (1994) 251–265.
[23] P.-Y. Lagrée, Removing the marching breakdown of the boundary-layer equations for mixed convection above a horizontal plate, Int. J. Heat Mass Transfer 44 (2001) 3359–3372.
[24] H. Schlichting, Boundary Layer Theory, seventh ed., McGraw-Hill, New York, 1979.
[25] D.B. Spalding, S.V. Patankar, Heat and Mass Transfer in Boundary Layers, Intertext Books, London, 1970.